Clinical Chemistry 55:5
955–963 (2009)

Tumor Cell Targeting Using Folate-Conjugated Fluorescent Quantum Dots and Receptor-Mediated Endocytosis

Er-Qun Song,[1] Zhi-Ling Zhang,[1] Qing-Ying Luo,[1] Wen Lu,[1] Yun-Bo Shi,[2] and Dai-Wen Pang[1*]

BACKGROUND: Luminescent nanobioprobes with cell-targeting specificity are likely to find important applications in bioanalysis, biomedicine, and clinical diagnosis. Quantum dots (QDs) are unique and promising materials for such a purpose because of their fluorescence and large surface area for attaching cell-targeting molecules.

METHODS: We produced water-dispersible QDs by coating hydrophobic QDs with small amphiphilic polyethylene glycol (PEG) molecules via hydrophobic interactions. We covalently coupled folate (FA) onto the water-dispersible PEG-coated QDs (PEG-QDs) to produce FA-coupled PEG-QDs (FA-PEG-QDs).

RESULTS: These FA-PEG-QD nanoparticles functioned as fluorescent nanobioprobes that specifically recognized folate receptors (FRs) overexpressed in human nasopharyngeal cells (KB cells) but not in an FR-deficient lung carcinoma cell line (A549 cells). Using confocal fluorescence microscopy, we demonstrated uptake of FA-PEG-QDs by KB cells but no uptake of folate-free PEG-QDs. The specificity of this receptor-mediated internalization was confirmed by comparing the uptake by KB vs A549 cells.

CONCLUSIONS: Our results suggest that such cell-targeting fluorescent nanobioprobes are potentially very powerful tools for recognizing target cells and delivering and tracking drugs and other therapeutic materials.

Quantum dots (QDs),[3] relatively new colloidal semiconductor nanocrystals, have been widely used as fluorescent probes in the fields of biomedical *(1–5)* and chemical-sensing and biosensing *(6, 7)* research owing to their stable and tunable multicolor fluorescence, broad absorption with narrow emission spectra, large molar extinction, high quantum yield, and high chemical stability *(1, 2, 8)*. In addition, the fluorescence of different colors from QDs can be excited with a single laser source of energy above the band gap of most blue-emitting QDs, allowing versatile multicolored complex detection. In some cases, particularly in live cell imaging for long periods of time and multicell imaging at a single time, these unique properties have obvious advantages over traditional organic fluorophores. Colloidal QDs are often prepared from organometallic precursors using high-temperature solution chemistry routes in the organic phase, producing QDs that cannot be used for biomedical research directly *(9, 10)*. These QDs are often capped to obtain water-dispersible QDs, and the most widely used surface-capping materials are either small molecule coordinating thiol-based ligands such as mercaptoacetic acid (MAA) *(2, 11–13)* or amphiphilic polymers *(3, 14–17)* and polysaccharide *(18)*. QDs capped with MAA and various other monothiols are small and can be derived using carbodiimide coupling chemistry, but they tend to aggregate rapidly due to weak ligand–QD interactions. In addition, the ionization state of the carboxylic acid group is critical to the water solubility of MAA-capped QDs, causing solution instability under even slightly acidic conditions *(12)*. In contrast, amphiphilic polymer–coated QDs benefit from high quantum yield and stability, but the polymeric shell produces large hydrodynamic diameters *(17)*, which could potentially interfere with the function of labeled biomolecules.

[1] College of Chemistry and Molecular Sciences, Key Laboratory of Analytical Chemistry for Biology and Medicine of the Ministry of Education and State Key Laboratory of Virology, Wuhan University, Wuhan, People's Republic of China; [2] Section on Molecular Morphogenesis, Program on Cell Regulation and Metabolism, National Institute of Child Health and Human Development, NIH, Bethesda, MD.

* Address correspondence to this author at: College of Chemistry and Molecular Sciences, Key Laboratory of Analytical Chemistry for Biology and Medicine of the Ministry of Education and State Key Laboratory of Virology, Wuhan University, Wuhan 430072, P. R. China. Fax +86-27-6875-4067; e-mail dwpang@whu.edu.cn.

Received June 30, 2008; accepted January 22, 2009.
Previously published online at DOI: 10.1373/clinchem.2008.113423

[3] Nonstandard abbreviations: QD, quantum dot; MAA, mercaptoacetic acid; FA, folate; FR, folate receptor; PEG, polyethylene glycol; PEG-QD, PEG-coated QD; FA-PEG-QD, folate-coupled PEG-QD; DCC, dicyclohexylcarbodiimide; NHS, *N*-hydroxysuccinimide; aminoPEG-2000, 1,2-distearoyl-sn-glycero-3-phosphatidyl-ethanolamine-*N*-[amino(polyethylene-glycol)2000; mPEG-750, 1,2-distearoyl-sn-glycero-3-phosphatidyl-ethanolamine-*N*-[methoxy(polyethyleneglycol)750; TEM, transmission electron microscopy; DLS, dynamic light scattering; AFM, atomic force microscopy; MTT, 3-(4,5-dimethylthiazlo-2-yl)-2,5-diphenyltetrazolium bromide.

Water-dispersible QDs with functional surface can be linked to antibodies, peptides, DNA, and small molecules to target specific cells for in vitro and in vivo applications *(19)*. Folate (FA), an essential precursor for the synthesis of nucleic acids and some amino acids, is not produced endogenously by mammalian cells and requires internalization by cells via either receptor-mediated endocytosis or nonspecific endocytosis *(20)*. Folate receptors (FRs), 38-kDa glycosyl-phosphatidyl-inositol–anchored glycoproteins, are overexpressed in many human cancer cells *(21)*, including malignancies of the ovary, mammary gland, lung, kidney, brain, prostate, nose, and throat, but minimally expressed in normal tissues *(22)*. FRs have a high affinity for FA, which results in efficient uptake of FA by FR-positive cells *(23)*. Both FA and its conjugate enter cells via endocytosis and have been used for targeted delivery of liposomes *(24)*, plasmid complexes *(25)*, nanoparticles *(26, 27)*, and anticancer drugs *(28)* to FR-positive cancer cells.

We were interested in developing simple, water-dispersible, stable FA-coupled quantum dot nanoparticles with a small size for targeting and recognizing/tracking live cells. Several articles on constructing such FA-coupled QD nanoparticles have been published *(17, 29–31)*. Some of them were made from MAA-capped QDs, which are not very stable, as mentioned above *(12)*; others have a large diameter *(17, 30, 31)*. Here, we capped QDs with amphiphilic polyethylene glycol (PEG) molecules of low molecular weight to produce stable, small, and high-quantum-yield water-dispersible PEG-coated QDs (PEG-QDs). These PEG-QDs were covalently conjugated with FA to produce FA-coupled PEG-QDs (FA-PEG-QDs). We report here the characteristics of these FA-PEG-QDs and their ability to specifically target cancer cells overexpressing FRs.

Materials and Methods

REAGENTS

Folate (molecular weight 440), DMSO, and MAA were purchased from Guoyaojituan; dicyclohexylcarbodiimide (DCC) and *N*-hydroxysuccinimide (NHS) from Sigma-Aldrich; 1,2-distearoyl-sn-glycero-3-phosphatidyl-ethanolamine-*N*-[amino(polyethylene-glycol)2000] (aminoPEG-2000) and 1,2-distearoyl-sn-glycero-3-phosphatidyl-ethanolamine-*N*-[methoxy(polyethylene glycol)750] (mPEG-750) from Avanti Polar Lipids Inc.; and KB and A549 cells from China Type Culture Collection. All the media used for cell culture were obtained from Gibco and purchased from Invitrogen Corp.

SYNTHESIS OF CdSe/ZnS QDs AND WATER-DISPERSIBLE FA-MAA-QDs

We synthesized monodisperse hydrophobic CdSe/ZnS QDs with a diameter of about 5 nm as described *(32)*, using trioctylphosphine oxide as the solvent in the synthesis. We prepared the water-dispersible FA-MAA-QDs according to a published procedure *(29)*. Briefly, a mixture of MAA and dried CdSe/ZnS QDs was first stirred vigorously for 1 h to prepare MAA-capped QDs via ligand exchange. The MAA-capped QDs were then activated with DCC and NHS for 30 min. Finally, the FA was added and stirred overnight to produce FA-MAA-QDs.

PREPARATION OF PEG-QDs

The water-dispersible PEG-QDs were prepared based on the method of Dubertret et al. *(3)* with some modifications. We used a molar ratio of 30% mPEG-1000 and 70% aminoPEG-2000 phospholipids. We dissolved the PEG and QDs at a 300:1 mol/L ratio in 10 mL chloroform. The chloroform was evaporated over a 30-min period using a circumrotate evaporation instrument, and the residue was dried by heating to 80 °C for 10 min. The dry film was resuspended by adding hot water (about 80 °C), followed by filtering with a 0.1-μm syringe filter to remove the large, hollow PEG micelles. We centrifuged the emulsion at 500 000*g* for 2 h with a Beckman ultracentrifuge and resuspended the pellet in 1 mL ultrapure water. This generated clear and stable PEG-QDs.

PREPARATION OF FA-PEG-QDs

Briefly, FA was activated with DCC and NHS at a 1:2:2 mol/L ratio in DMSO for 12 h and filtered with a syringe filter (pore size 0.2 μm). The PEG-QDs were added to the solution at a molar ratio of 10:1 (FA:PEG-QDs). After reacting for 4 h at room temperature in the dark, the reactants were dialyzed against a 0.05 mol/L sodium bicarbonate buffer (SpectraPor6; molecular weight cutoff 1000). It is important to note that the addition of DCC and NHS to folate forms a highly reactive intermediate (FA-NHS), which can subsequently react with the free amino group present in PEG-QDs to form the resulting FA-PEG-QDs, as shown in Fig. 1.

TRANSMISSION ELECTRON MICROSCOPY IMAGING

We examined the size and the morphology of the FA-PEG-QDs by transmission electron microscopy (TEM) using a JEOL JEM-100CX with 1 drop of the FA-PEG-QD solution mounted on a thin film of amorphous carbon deposited on a copper grid.

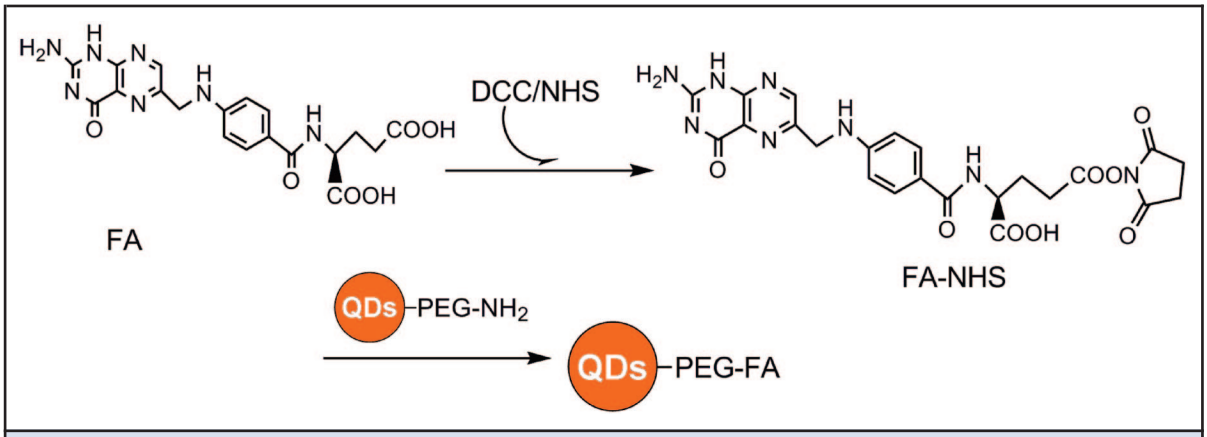

Fig. 1. Synthesis of FA-PEG-QDs.
FA was first activated with DCC/NHS to form a reactive intermediate (FA-NHS). The H_2N-PEG-QDs reacted with the FA-NHS to produce FA-PEG-QDs.

DYNAMIC LIGHT SCATTERING MEASUREMENT

We measured the effective size and size distribution of the FA-PEG-QD suspensions by dynamic light scattering (DLS) using a Zetasizer Nano ZS90 (Malvern Instruments). FA-PEG-QD nanoparticles were dispersed in 1 mL ultrapure water. The solution was filtered through a 0.1-μm syringe filter membrane to remove any impurities and then directly analyzed.

ATOMIC FORCE MICROSCOPY IMAGING

We characterized the appearance and monodispersity of the FA-PEG-QD nanoparticles by atomic force microscopy (AFM) using a PicoScan atomic force microscope (Molecular Imaging). Sample solution (10 μL) was dropped onto a freshly cleaved ruby muscovite mica substrate (Digital Instruments) and allowed to dry for about 2 h. Freshly prepared samples were mounted on the AFM stage and imaged under MAC Mode in air (relative humidity 40%–50%, approximately 25 °C) using MAClever type II probes (spring constant 2.8 N/m, resonant frequency approximately 85 kHz; Molecular Imaging). The scan rate was about 1.5 line/s.

MEASUREMENT OF FLUORESCENCE SPECTRA

We measured the fluorescence spectra of the free hydrophobic QDs, PEG-QDs, and FA-PEG-QDs using a PerkinElmer LS 55 fluorescence spectrometer with a 388-nm laser for excitation and analyzed the spectra using FL WinLab 4.00.02 software (PerkinElmer).

MEASUREMENT OF QUANTUM YIELD

We measured the quantum yields of the free hydrophobic QDs, PEG-QDs, and FA-PEG-QDs using a PerkinElmer LS 55 fluorescence spectrometer according to a published procedure *(33)*, using Rhodamine 640 dissolved in absolute ethanol as the reference standard (quantum yield 100%). We calculated the relative quantum yield of the QDs from the following equation:

$$\Phi_x = \Phi_{ST}(m_x/m_{ST})(\eta_x/\eta_{ST})^2$$

where the subscripts *ST* and *x* denote the standard and tested sample, respectively, Φ is the fluorescence quantum yield, *m* is the slope from the plot of the integrated fluorescence intensity vs the absorbance of the sample or the standard at different concentrations, and η is the refractive index of the solvent.

MEASUREMENT OF THE ZETA POTENTIAL

The ζ potential is a measure of the potential at the interface between a solid surface and the liquid medium. We used a Zetasizer Nano ZS90 (Malvern Instruments) to measure the ζ potential of PEG-QD and FA-PEG-QD nanoparticles dispersed in 1 mL of ultrapure water.

QUANTIFICATION OF FA ON FA-PEG-QDs

We measured the amount of folate conjugated to the QDs using a fluorescamine assay *(34)*. A series of standard solutions of free FA were reacted with 1 mL of 5×10^{-4} mol/L fluorescamine, and the integrated fluorescence intensity of their reaction product from 460 to 485 nm was calculated to plot a calibration curve of fluorescence intensity vs the concentration of FA. Subsequently, we mixed the FA-PEG-QD solution at indicated concentrations of QDs with fluorescamine and similarly determined the emission intensity. The concentration of FA in the solution of FA-PEG-QDs was obtained according to the calibration curve. Finally, we

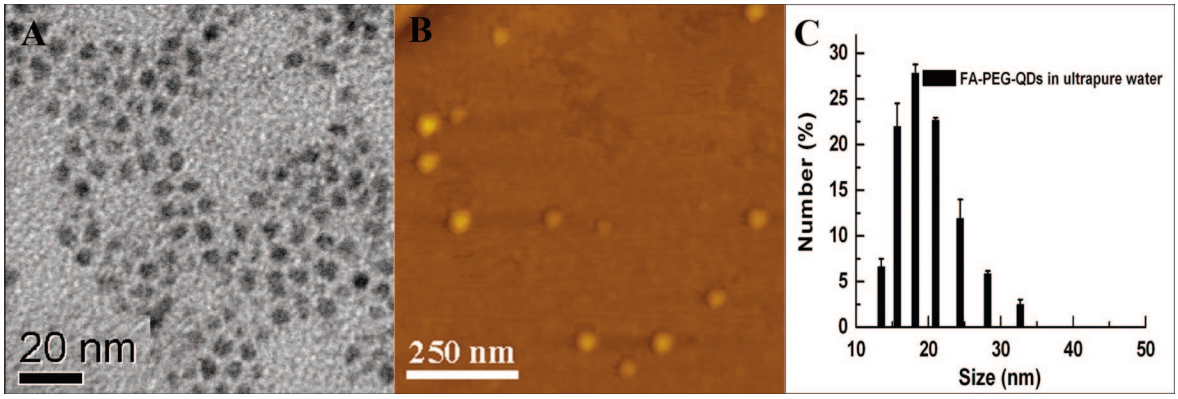

Fig. 2. Size characterization of FA-PEG-QD nanobioprobes.

(A), TEM image showing homogenous size distribution. (B), AFM image showing spherical shape of FA-PEG-QD nanoparticles. (C), DLS data showing the size distribution of FA-PEG-QDs in ultrapure water. The vertical axis shows the number of FA-PEG-QD nanoparticles with the diameters on the horizontal axis. The average diameter is 22 (10) nm.

calculated the number of FA molecules on a single of FA-PEG-QD according to the following equation:

$$N_{FA} = C_{FA}/C_{QDs}$$

where N_{FA} is the number of FA molecules on each FA-PEG-QD, C_{FA} is the concentration of FA in the tested FA-PEG-QD solution, and C_{QDs} is the concentration of QDs in the tested FA-PEG-QD solution.

CELL CULTURE

The FR-overexpressing human nasopharyngeal cell line (KB) and FR-deficient lung carcinoma cell line (A549) were grown in folate-free RPMI 1640 medium with 10% fetal bovine serum, 100 U/mL penicillin G sodium, and 0.1 g/L streptomycin sulfate. To study the uptake and imaging of the conjugated FA, we seeded the KB and A549 cell lines on a 35-mm culture glass plate at a density 3×10^5 cells/well. After 36 h of incubation, we rinsed the cells with sterile PBS and added 2 mL of the corresponding fresh media containing the indicated concentrations of FA-PEG-QDs to the plates. Plates were returned to the incubator (37 °C, 5% CO_2) for the indicated incubation period. After each indicated time interval of incubation, the plates were taken out and rinsed several times with sterile PBS, and 2 mL of fresh serum-free medium was added. After incubation for another 10 min at 37 °C, the plates were directly imaged under an inversion fluorescence microscope (Nikon ECLIPSE TE2000-U) or a confocal laser scanning fluorescence microscope (Leica TCS-SP2). To confirm receptor-mediated uptake, competition experiments were conducted where the KB cells were pretreated for 1 h with 2 mL of 1 mmol/L free FA solution before FA-PEG-QD treatment.

CELL VIABILITY ASSAY

We tested the effect of FA-MAA-QDs and FA-PEG-QDs on KB cell proliferation using an MTT [3-(4,5-dimethylthiazlo-2-yl)-2,5-diphenyltetrazolium bromide] cell viability assay *(35)*. We added 200 μL of KB cells suspended in FA-deficient RPMI 1640 to each well of a 96-well plate (4×10^4 cells/mL). The cells were incubated for 24 h in an incubator (37 °C, 5% CO_2) and for another 24 h after the culture medium was replaced with 200 μL FA-deficient RPMI 1640 containing the FA-PEG-QDs and FA-MAA-QDs at indicated concentrations. Then we added 20 μL of 5 g/L MTT solution to each well. The cells were further incubated for 4 h, the culture medium containing MTT was removed, and 150 μL DMSO was added to each well. The resulting mixture was mixed for approximately 5 min at room temperature. The absorbance (A) of the mixture was measured at 570 nm using a Microplate Reader Model 550 (Bio-Rad). The control experiments were carried out in the same manner as described above, except that no FA-PEG-QDs or FA-MAA-QDs were added.

Results and Discussion

SIZE CHARACTERIZATION

We first determined the size of the FA-PEG-QDs by transmission electron microscopy. The TEM image showed that the FA-PEG-QDs appeared as particles of about 5 nm in diameter (Fig. 2A). AFM analysis clearly showed that the FA-PEG-QDs were spherical in shape with a mean (SD) height of 7 (2) nm (Fig. 2B). The larger diameter determined by AFM was because the QD core was coated with a PEG shell coupled with

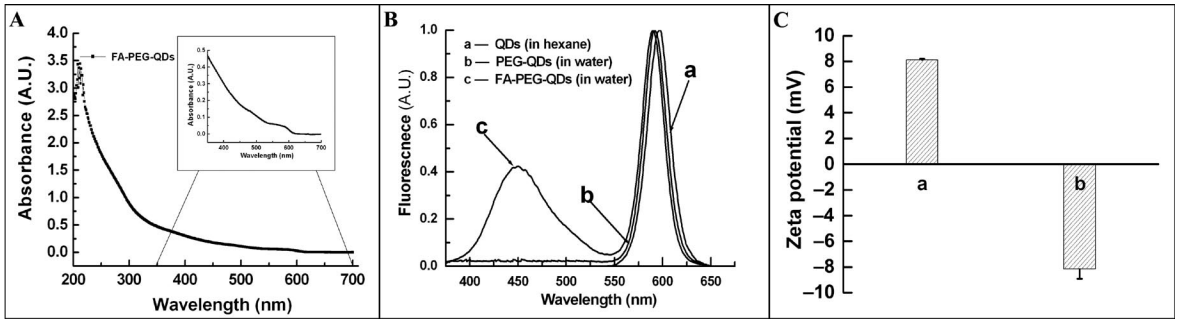

Fig. 3. (A), Absorption spectrum of FA-PEG-QDs dispersed in ultrapure water.

The inset shows the first exciton absorption peak of the QDs. (B), Normalized fluorescence spectra of free hydrophobic QDs dispersed in n-hexane (curve a), PEG-QDs (curve b), and FA-PEG-QDs (curve c) dispersed in ultrapure water. (C), Zeta potential distribution of PEG-QD (a) and FA-PEG-QD (b) nanoparticles in ultrapure water. A.U., arbitrary units.

FA ligands. Both analyses showed that these FA-PEG-QD nanoparticles had good uniformity in size and monodispersity.

DLS was then used to measure the size distribution of the prepared FA-PEG-QD nanoparticles in suspension. Fig. 2C shows the effective size as well as the size distributions of the FA-PEG-QDs suspended in ultrapure water. The results demonstrated that the FA-PEG-QDs in ultrapure water had a relatively narrow size distribution, ranging from 13 to 32 nm in diameter. The mean diameter of the FA-PEG-QDs was 22 (10) nm. The larger diameter observed from DLS analysis included not only the QD core, which is measurable using TEM, but also the hydrodynamic diameter from the PEG coating, the covalently linked FA molecules, and the hydrated layer.

OPTICAL CHARACTERIZATION AND ZETA POTENTIAL OF FA-PEG-QDs

We examined the optical characteristics of the QD nanoparticles by measuring the absorption and fluorescence spectra. Fig. 3A shows the absorption spectrum of FA-PEG-QDs in ultrapure water. As shown in Fig. 3B, the PEG-QDs had a fluorescence emission peak at 594 nm, close to that of the same free hydrophobic QDs in hexane (595 nm). The fluorescence emission peak of the FA-PEG-QDs (593 nm) was slightly blue-shifted compared to that of the PEG-QDs (594 nm) and free QDs (595 nm), probably owing to the ligands on the surface of the QD nanoparticles and the difference in the QD environments—n-hexane for free hydrophobic QDs and water for the PEG-coated QDs. A second fluorescence emission peak at 450 nm was observed for the FA-PEG-QDs owing to the fluorescence spectrum of FA conjugated to the QD nanoparticles, which clearly demonstrated that the FA had been successfully coupled to the QDs. We measured photoluminescence quantum yields of the free hydrophobic QDs, PEG-QDs, and FA-PEG-QDs using Rhodamine 640 as a reference standard. The mean (SD) quantum yields of the original hydrophobic QDs, PEG-QDs, and FA-PEG-QDs were 34.8% (3%), 12.1% (1.6%), and 7.2% (2.2%), respectively. Thus, the results showed that the quantum yield of PEG-QDs was about 35% that of the original hydrophobic QDs, whereas the quantum yield of FA-PEG-QDs was about 21% that of the original hydrophobic QDs, indicating that the modified QDs retained substantial fluorescent properties of the original QDs.

To investigate the uniformity of the coupling of FA to QDs, we measured the ζ potential of the FA-PEG-QDs. The ζ potential is a measure of the potential at the interface between a solid surface and the liquid medium. As FA contains 2 carboxy groups, 1 carboxy group would remain after the FA covalently binds to the PEG-QDs due to the inert property of the α-carboxyl group and the stereohindrance effect. Consequently, the ζ potential of the FA-PEG-QDs would be shifted negatively compared with FA-free PEG-QDs. Indeed, we found that PEG-QDs had a negative ζ potential, whereas FA-PEG-QDs had a positive ζ potential (Fig. 3C). This indicated that the FA had been conjugated to the PEG-QDs, consistent with the fluorescence emission spectrum of the FA-PEG-QDs. The sharp peak in the ζ potential distribution of the nanoparticles indicated that each FA-PEG-QD had a similar number of coupled FA molecules.

QUANTIFICATION OF FA ON THE QDs, STABILITY AND CELL TOXICITY OF FA-PEG-QDs

We carried out a fluorescamine assay *(34)* to determine the number of FA molecules conjugated to the QDs.

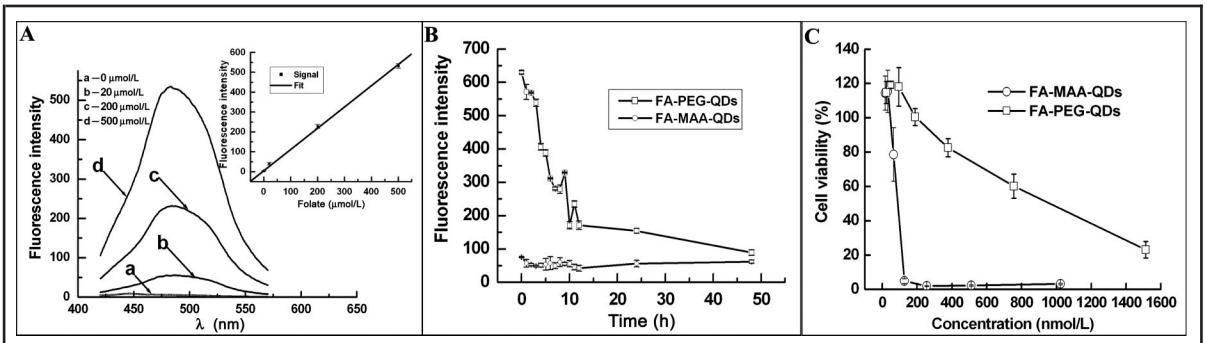

Fig. 4. (A), Fluorescamine assay to measure the number of FA molecule per QD.

Emission spectra of FA at indicated concentrations were determined after treatment with fluorescamine (380 nm excitation, 480 nm emission). Inset: integrated fluorescence intensity of these samples from 460 to 485 nm (horizontal axis) was plotted against FA concentration (vertical axis). (B), Fluorescence intensity of FA-PEG-QDs (□) and FA-MAA-QDs (○) with a concentration of 200 nmol/L in FA-deficient RPMI 1640 culture medium as a function of time. At the indicated time points, the samples were excited with 388 nm light and the fluorescence intensity of QDs was recorded. (C), Growth inhibition assay (MTT assay) of KB cells treated with different concentrations of FA-PEG-QD (□) and FA-MAA-QD (○) nanoparticles. In our experiments, there was more than 100% survival at low concentrations (<200 nmol/L for FA-PEG-QDs; <50 nmol/L for FA-MAA-QDs), as the cell number exceeded that for the control due to some cell proliferation under the assay conditions.

Fluorescamine can react with all substances containing primary amino groups, and each coupled FA molecule on the QDs has 1 primary amino group. This reaction yields intensely fluorescent products (excitation at 380 nm, emission at 480 nm) with a fluorescence emission peak at 480 nm (Fig. 4A). According to the calibration curve ($y = 4.903 + 1.069x$, $r = 0.9986$) plotted based on the integrated fluorescence intensity around 480 nm of the reaction product vs the concentration of FA, we obtained different concentrations (9.09×10^{-4}, 5.04×10^{-4}, 2.01×10^{-4} mol/L, respectively) of FA corresponding to different concentrations (3.0×10^{-5}, 1.5×10^{-5}, 0.75×10^{-5} mol/L) of QDs in the tested FA-PEG-QDs solution. According to Equation 2, approximately 30 (4) FA molecules were coupled to 1 FA-PEG-QD.

To be useful for cell targeting, the QD moiety of the FA-PEG-QDs would need to have strong and stable fluorescence in aqueous solutions. Thus, we compared the stability of the fluorescence intensity of QDs in the FA-PEG-QDs with FA-MAA-QDs in the FA-deficient RPMI 1640 culture medium. The results showed that the fluorescence intensity from FA-MAA-QDs was very unstable in the aqueous culture medium, with faint fluorescence even at the earlier point of measurement (Fig. 4B). The fluorescence intensity of FA-PEG-QDs was more than 10 times stronger than that of the FA-MAA-QDs within the first few hours and remained stronger even at 48 h. These results demonstrate that FA-PEG-QDs are superior to FA-MAA-QDs for applications in biomedical research. It should be noted that with similar amounts of QDs used, the initial fluorescence intensity of both FA-PEG-QDs and FA-MAA-QDs should be almost the same. Under the experimental conditions, the fluorescence intensity of the FA-MAA-QDs was so unstable that it decayed to near the basal value at the earliest possible measurable time point. In contrast, the fluorescence intensity of the FA-PEG-QDs was much more stable and decayed by about half fluorescence intensity at about 9 h.

It is well known that QDs have a certain extent of toxicity to cells, which limits their applications. We therefore examined the toxicity of FA-MAA-QDs and FA-PEG-QDs on KB cells using an MTT cell viability assay. The cell viability was determined according to the following equation:

$$\text{Cell viability (\%)} = (A_{\text{treated}}/A_{\text{control}}) \times 100$$

where A_{control} was obtained in the absence of QDs and A_{treated} was obtained in the presence of FA-PEG-QDs or FA-MAA-QDs. As shown in Fig. 4C, FA-MAA-QDs had a severe toxic effect on KB cells at 100 nmol/L, whereas FA-PEG-QDs had little effect on the KB cells. Only at 200 nmol/L or higher did FA-PEG-QDs have any toxic effect on the KB cells. Thus, these results indicate that FA-PEG-QDs are superior to FA-MAA-QDs for live cell targeting. The data in Fig. 4C also suggest that not only do both FA-MAA-QDs and FA-PEG-QDs have no cytotoxicity, but they even promote the growth of cells when their concentration is lower than 50 nmol/L. The increase in cell viability might be related to the effect of nanomaterials on organisms,

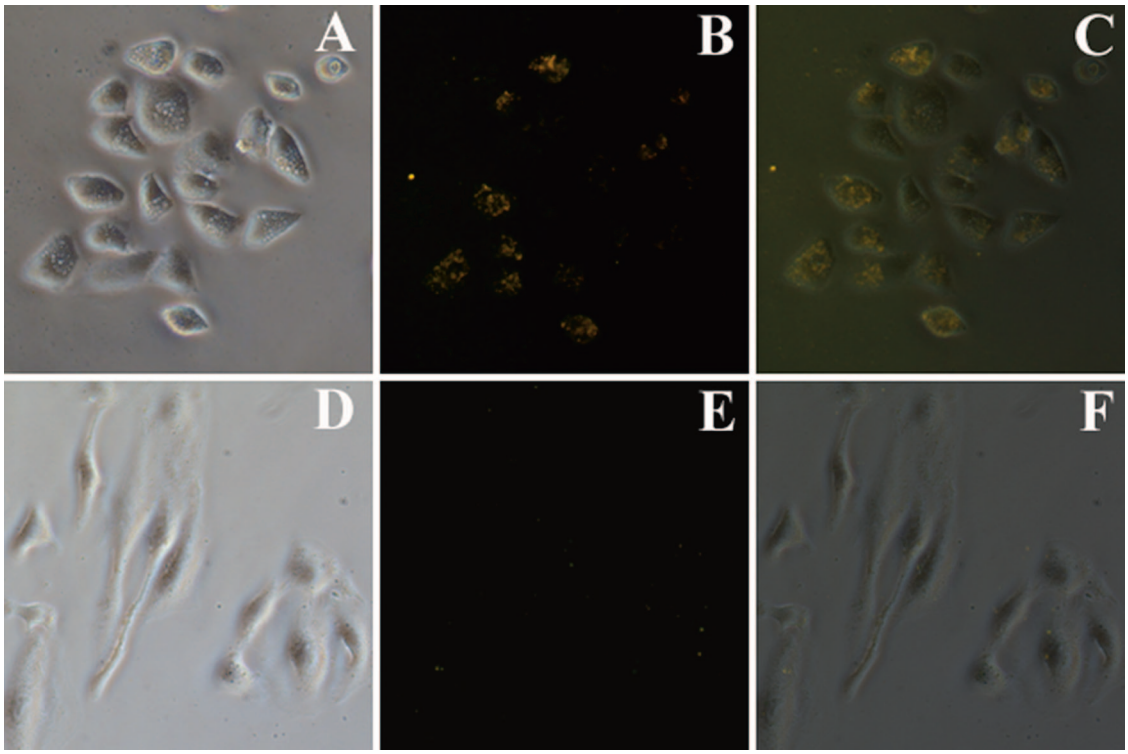

Fig. 5. Microscopic images of tumor cells after incubation with FA-PEG-QD nanobioprobes for 2 h (objective 20×).
(A), Bright field of KB cells. (B), Orange fluorescence from FA-PEG-QDs bound to KB cells. (C), Merged photo of (A) and (B). (D), Bright field of A549 cells. (E), Fluorescence field of A549 cells, no fluorescence found except some nonspecific signals. (F), Merged photo of (D) and (E).

which is extremely complicated. According to previous reports on the effect of QDs on cell viability *(36–40)*, factors such as the size, shape, and type of QDs; surface charge and functional groups on QDs; concentration of QDs; and type of cells tested may affect cell viability. In some cases, QDs will restrain the proliferation of cells *(36, 40)*, and in some cases, QDs have no cytotoxicity and even promote the growth of cells *(37, 38)*. It is difficult, however, to explain why QDs promote the growth of cells at present.

FA-PEG-QDs SPECIFICALLY TARGETING FR-POSITIVE KB CELLS AND INTERNALIZED BY KB CELLS

FA has a high affinity for FR and can be internalized though FR-mediated endocytosis. To investigate whether the FA on FA-PEG-QDs can mediate specific cell targeting, we incubated the FR-positive KB and FR-negative A549 cells with 100 nmol/L FA-PEG-QDs for 2 h and then washed the cells to remove unbound FA-PEG-QDs. Fluorescence imaging analysis showed strong orange fluorescence from FA-PEG-QDs on the KB cells (Fig. 5, A–C) but not on the A549 cells (Fig. 5, D–F), demonstrating that the FA-PEG-QDs specifically target the FR-positive tumor cells.

To study the intracellular uptake of the FA-PEG-QDs, KB and A549 cells were treated with 200 nmol/L FA-PEG-QDs for 4 h, and the cells were examined under a confocal laser-scanning microscope. As shown in Fig. 6A, strong fluorescence from the FA-PEG-QDs was found inside the KB cells due to internalization of the FA-PEG-QDs into the KB cells. In contrast, KB cells incubated with PEG-QDs without FA (Fig. 6C) and A549 cells incubated with FA-PEG-QDs had only faint fluorescence inside the cells (Fig. 6B). These weak background signals were likely due to nonspecific endocytosis that occurs in all cell types, since they were independent of either FA (Fig. 6C) or FRs (Fig. 6B). Consistently, when KB cells were first incubated with excess free FA to block FRs and subsequently incubated with FA-PEG-QDs, the intracellular fluorescence was reduced to similarly weak levels (Fig. 6D). Thus, we conclude that FA-PEG-QDs not only specifically target FR-positive cells, but are also internalized through receptor-mediated endocytosis, suggesting that FA-

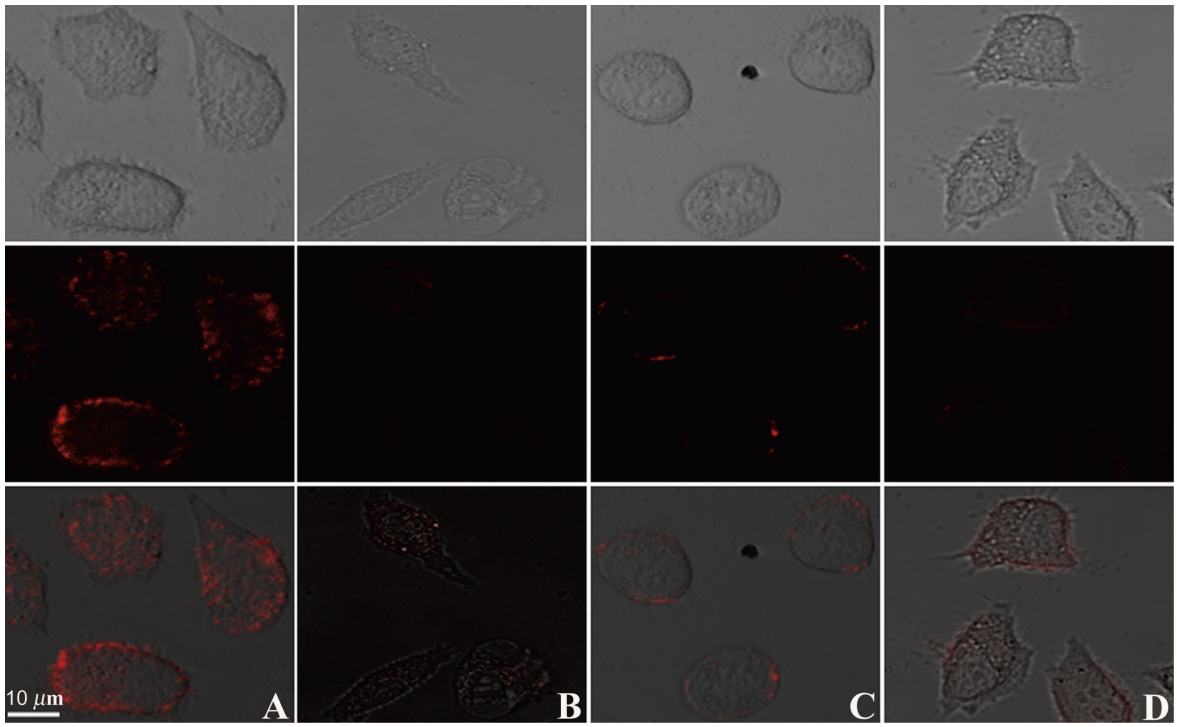

Fig. 6. Confocal microscopic analysis of cells incubated with FA-PEG-QD and FA-free PEG-QD nanoparticles.

Cells were grown on glass slides inserted in Petri dishes with glass surface, incubated for 4 h with indicated QD preparations, and washed for microscopic observation. (A), FA-PEG-QDs with KB cells. (B), FA-PEG-QDs with A549 cells. (C), FA-free PEG-QDs with KB cells. (D), KB cells incubated with free FA for 1 h before exposure to FA-PEG-QDs for 4 h. The top channel shows the transmission images, the middle channel shows the fluorescence, and the bottom channel shows the merged photo of the top and middle channels. Note that because the pictures in Fig. 6 were obtained with a confocal microscope in false color, the color of the QDs was different from that in Fig. 5, where the photos were taken with a fluorescence microscope equipped with a digital camera in true color.

PEG-QDs are potentially powerful tools for targeting cancer cells for in vivo labeling/imaging (because of fluorescence), delivering therapeutic compounds (because of internalization), and tracking the targeting drugs (because of both fluorescence and internalization).

The FA-PEG-QD nanoparticles have a homogeneous size distribution and FA coupling, and retain the fluorescent properties of the parental QDs. With these properties, they are superior to other reported FA-coupled QDs or nanospheres for biomedical applications requiring aqueous conditions. These FA-PEG-QD nanobioprobes also show cell-targeting specificity through cell-surface FRs and internalization through FR-mediated endocytosis. We believe that the FA-PEG-QD nanobioprobes, with their superior properties of fluorescence, specificity, monodispersity, and smaller diameter for endocytosis, would be ideal for biomedical applications such as specifically killing cancer cells by adding antitumor drugs to the FA-PEG-QDs.

Author Contributions: *All authors confirmed they have contributed to the intellectual content of this paper and have met the following 3 requirements: (a) significant contributions to the conception and design, acquisition of data, or analysis and interpretation of data; (b) drafting or revising the article for intellectual content; and (c) final approval of the published article.*

Authors' Disclosures of Potential Conflicts of Interest: *Upon manuscript submission, all authors completed the Disclosures of Potential Conflict of Interest form. Potential conflicts of interest:*

Employment or Leadership: None declared.
Consultant or Advisory Role: None declared.
Stock Ownership: None declared.
Honoraria: None declared.
Research Funding: The National Key Scientific Program (973)—Nanoscience and Nanotechnology (2006CB933100), the Science

Fund for Creative Research Groups of NSFC (20621502), the 863 Program (2006AA03Z320), the National Natural Science Foundation of China (30570490 and 20833006), the Ministry of Education (306011 and IRT0543), and the Intramural Research Program of the National Institute of Child Health and Human Development, NIH, USA.

Expert Testimony: None declared.

Role of Sponsor: The funding organizations played no role in the design of study, choice of enrolled patients, review and interpretation of data, or preparation or approval of manuscript.

Acknowledgments: We thank Min Liu and Yang Wang for their kind help.

References

1. Bruchez M Jr, Moronne M, Gin P, Weiss S, Alivisatos AP. Semiconductor nanocrystals as fluorescent biological labels. Science (Wash DC) 1998; 281:2013–6.
2. Chan WCW, Nie SM. Quantum dot bioconjugates for ultrasensitive nonisotopic detection. Science (Wash DC) 1998;281:2016–8.
3. Dubertret B, Skourides P, Norris DJ, Noireaux V, Brivanlou AH, Libchaber A. In vivo imaging of quantum dots encapsulated in phospholipid micelles. Science (Wash DC) 2002;298:1759–62.
4. Wu X, Liu H, Liu J, Haley KN, Treadway JA, Larson JP, et al. Immunofluorescent labeling of cancer marker Her2 and other cellular targets with semiconductor quantum dots. Nat Biotechnol 2003; 21:41–6.
5. Song EQ, Wang GP, Xie HY, Zhang ZL, Hu J, Peng J, et al. Visual recognition and efficient isolation of apoptotic cells with fluorescent-magnetic-biotargeting multifunctional nanospheres. Clin Chem 2007;53:2177–85.
6. Zhang CY, Yeh HC, Kuroki MT, Wang TH. Single-quantum-dot-based DNA nanosensor. Nat Mater 2005;4:826–31.
7. Snee PT, Somers RC, Nair G, Zimmer JP, Bawendi MG, Nocera DG. A ratiometric CdSe/ZnS nanocrystal pH sensor. J Am Chem Soc 2006;128: 13320–1.
8. Dabbousi BO, Rodriguez-Viejo J, Mikulec FV, Heine JR, Mattoussi H, Ober R, et al. (CdSe)ZnS core-shell quantum dots: synthesis and characterization of a size of highly luminescent nanocrystallites. J Phys Chem B 1997;101:9463–75.
9. Peng ZA, Peng X. Formation of high-quality CdTe, CdSe, and CdS nanocrystals using CdO as precursor. J Am Chem Soc 1993;123:183–4.
10. Murray CB, Norris DJ, Bawendi MG. Synthesis and characterization of nearly monodisperse CdE (E=sulfur, selenium, tellurium) semiconductor nanocrystallites. J Am Chem Soc 1993; 115:8706–15.
11. Mattoussi H, Mauro JM, Goldman ER, Anderson GP, Sundar VC, Mikulec FV, et al. Self-assembly of CdSe-ZnS quantum dot bioconjugates using an engineered recombinant protein. J Am Chem Soc 2000;122:12142–50.
12. Aldana J, Wang YA, Peng X. Photochemical instability of CdSe nanocrystals coated by hydrophilic thiols. J Am Chem Soc 2001;123:8844–50.
13. Algar WR, Krull UJ. Adsorption and hybridization of oligonucleotides on mercaptoacetic acid-capped CdSe/ZnS quantum dots and quantum dot-oligonucleotide conjugates. Langmuir 2006; 22:11346–52.
14. Dahan M, Levi S, Luccardini C, Rostaing P, Riveau B, Triller A. Diffusion dynamics of glycine receptors revealed by single-quantum dot tracking. Science (Wash DC) 2003;302:442–5.
15. Medintz I, Uyeda H, Goldman E, Mattoussi H. Quantum dot bioconjugates for imaging, labeling and sensing. Nat Mater 2005;4:435–46.
16. Smith AM, Duan H, Rhyner, MN, Ruan G, Nie S. A systematic examination of surface coatings on the optical and chemical properties of semiconductor quantum dots. Phys Chem Chem Phys 2006;8:3895–903.
17. Schroeder JE, Shweky I, Shmeeda H, Banin U, Gabizon A. Folate-mediated tumor cell uptake of quantum dots entrapped in lipid nanoparticles. J Control Release 2007;124:28–34.
18. Xie M, Liu HH, Chen P, Zhang ZL, Wang XH, Xie ZX, et al. CdSe/ZnS-labeled carboxymethyl chitosan as a bioprobe for live cell imaging. Chem Commun 2005;44:5518–20.
19. Jamieson T, Bakhshi R, Petrova D, Pocock R, Imani M, Seifalian AM. Biological applications of quantum dots. Biomaterials 2007;28:4717–32.
20. Sabharanjak S, Mayor S. Folate receptor endocytosis and trafficking. Adv Drug Delivery Rev 2004; 56:1099–109.
21. Toffoli G, Cernigoi C, Russo A, Gallo A, Bagnoli M, Boiocchi M. Overexpression of folate binding protein in ovarian cancers. Int J Cancer 1997;74: 193–8.
22. Weitman SD, Lark RH, Coney LR, Fort DW, Frasca V, Zurawski VR Jr, Kamen BA. Distribution of the folate receptor GP38 in normal an malignant cell lines and tissues. Cancer Res 1992;52:3396–401.
23. Elnakat H, Ratnam M. Distribution, functionality, and gene regulation of folate receptor isoforms: implications in targeted therapy. Adv Drug Delivery Rev 2004;56:1067–84.
24. Leamon CP, Cooper SR, Hardee GE. Folate-liposome-mediated antisense oligodeoxynucleotide targeting to cancer cells: evaluation in vitro and in vivo. Bioconjugate Chem 2003;14:738–47.
25. Zhou W, Yuan X, Wilson A, Yang L, Mokotoff M, Pitt B, et al. Efficient intracellular delivery of oligonucleotides formulated in folate receptor-targeted lipid vesicles. Bioconjugate Chem 2002; 13:1220–5.
26. Sonvico F, Mornet S, Vasseur S, Dubernet C, Jaillard D, Degrouard J, et al. Folate-conjugated iron oxide nanoparticles for solid tumor targeting as potential specific magnetic hyperthermia mediators: synthesis, physicochemical characterization, and in vitro experiments. Bioconjugate Chem 2005;16:1181–8.
27. Dixit V, Van den Bossche J, Sherman DM, Thompson DH, Andres RP. Synthesis and grafting of thioctic acid-PEG-folate conjugates onto Au nanoparticles for selective targeting of folate receptor-positive tumor cells. Bioconjugate Chem 2006;17:603–9.
28. Leamon CP, Reddy JA. Folate-targeted chemotherapy. Adv Drug Delivery Rev 2004;56:1127–41.
29. Bharali DJ, Lucey DW, Jayakumar H, Pudavar HE, Prasad PN. Folate-receptor-mediated delivery of InP quantum dots for bioimaging using confocal and two-photon microscopy. J Am Chem Soc 2005;127:11364–71.
30. Zhang Y, Huang N. Intracellular uptake of CdSe-ZnS/polystyrene nanobeads. J Biomed Mater Res B Appl Biomater 2006;76:161–8.
31. Xie HY, Zuo C, Liu Y, Zhang ZL, Pang DW, Li XL. Cell-targeting multifunctional nanospheres with both fluorescence and magnetism. Small 2005;1: 506–9.
32. Xie HY, Liang JG, Liu Y, Zhang ZL, He ZK, Lu ZX, et al. Preparation and characterization of overcoated II-VI quantum dots. J Nanosci Nanotechnol 2005;5:880–6.
33. Qu LW, Peng XG. Control of photoluminescence properties of CdSe nanocrystals in growth. J Am Chem Soc 2002;124:2049–55.
34. Udenfriend S, Stein S, Böhlen P, Dairman W, Leimgruber W, Weigele M. Fluorescamine: a reagent for assay of amino acids, peptides, proteins, and primary amines in the picomole range. Science (Wash DC) 1972;178:871–2.
35. Marks DC, Belov L, Davey MW, Davey RA, Kidman AD. The MTT cell viability assay for cytotoxicity testing in multidrug-resistant human leukemic cells. Leuk Res 1992;16:1165–73.
36. Shiohara A, Hoshino A, Hanaki K, Suzuki K, Yamamoto K. On the cyto-toxicity caused by quantum dots. Microbiol Immunol 2004;48:669–75.
37. Derfus AM, Chan WCW, Bhatia SN. Probing the cytotoxicity of semiconductor quantum dots. Nano Lett 2004;4:11–8.
38. Hoshino A, Fujioka K, Oku T, Suga M, Sasaki YF, Ohta T, et al. Physicochemical properties and cellular toxicity of nanocrystal quantum dots depend on their surface modification. Nano Lett 2004;4:2163–9.
39. Kirchner C, Liedl T, Kudera S, Pellegrino T, Javier AM, Gaub HE, et al. Cytotoxicity of colloidal CdSe and CdSe/ZnS nanoparticles. Nano Lett 2005;5: 331–8.
40. Zhang YB, Chen W, Zhang J, Liu J, Chen GP, Pope C. In vitro and in vivo toxicity of CdTe nanoparticles. J Nanosci Nanotechnol 2007;7:497–503.